Synthesis and characterization of band gap-reduced ZnO:N and ZnO:(Al,N) films for photoelectrochemical water splitting

Sudhakar Shet[a)]
National Renewable Energy Laboratory, Golden, Colorado 80401; and
New Jersey Institute of Technology, Newark, New Jersey 07102

Kwang-Soon Ahn
Energy & Environment Laboratory, Samsung Advanced Institute of Technology, Yongin-si, Gyeonggi-do 446-712, Republic of Korea

Todd Deutsch and Heli Wang
National Renewable Energy Laboratory, Golden, Colorado 80401

Nuggehalli Ravindra
New Jersey Institute of Technology, Newark, New Jersey 07102

Yanfa Yan,[b)] John Turner,[c)] and Mowafak Al-Jassim
National Renewable Energy Laboratory, Golden, Colorado 80401

(Received 13 May 2009; accepted 7 August 2009)

ZnO thin films with significantly reduced band gaps were synthesized by doping N and codoping Al and N at 100 °C. All the films were synthesized by radiofrequency magnetron sputtering on F-doped tin-oxide-coated glass. We found that codoped ZnO:(Al,N) thin films exhibited significantly enhanced crystallinity compared with ZnO doped solely with N, ZnO:N, at the same growth conditions. Furthermore, annealed ZnO:(Al,N) thin films exhibited enhanced N incorporation over ZnO:N films. As a result, ZnO:(Al,N) films exhibited better photocurrents than ZnO:N films grown with pure N doping, suggesting that charge-compensated donor–acceptor codoping could be a potential method for band gap reduction of wide-band gap oxide materials to improve their photoelectrochemical performance.

I. INTRODUCTION

Transition-metal oxides are potential candidates for photoelectrochemical (PEC) H_2 production from water.[1,2] However, to date, only TiO_2 has received extensive attention.[3–6] ZnO has similar band gap and band-edge positions compared with TiO_2,[1] but ZnO has a direct band gap and higher electron mobility than TiO_2.[7] Thus, the PEC property of ZnO also needs to be studied.[8] Like TiO_2, the band gap of ZnO (3.3 eV) is too large to effectively use visible light.[3] Therefore, it is critical to reduce the band gap of ZnO.

To date, impurity incorporation has been the main method of reducing the band gap of TiO_2. It has been reported that N, C, and S doping can successfully narrow the band gap of TiO_2 and push the photoresponse into the long-wavelength region.[3–6] Although band gap reduction of TiO_2 has been extensively studied, very limited research exists on band gap narrowing of ZnO by impurity incorporation. Significant amounts of N can be incorporated into ZnO and WO_3 only at low temperatures.[9,10] However, films grown at low temperature usually exhibit poor crystallinity, which is extremely detrimental to PEC performance. This dilemma hinders the PEC performance of N-incorporated ZnO and WO_3 films. A possible cause for the inferior crystallinity may be uncompensated charged N atoms. This problem could be overcome by charge-compensated donor–acceptor doping, such as codoping ZnO with Al and N. Furthermore, incorporating (Al,N) pairs is easier than incorporating sole N atoms because of donor–acceptor interaction.[11–13] The Al and N codoped ZnO films have been synthesized by many groups; however, to date, these studies have focused mostly on p-type doping, and thus, the doping concentration was usually low and the band gap of ZnO was not heavily affected.[14–18] The effect of passive codoping of Al and N in ZnO thin films on PEC performance has not been investigated. Zn atoms always combine preferentially with O, rather than with N.

In this paper, we report on the synthesis of ZnO:N and ZnO:(Al,N) thin films by reactive radiofrequency (RF)

Address all correspondence to these authors.
[a)]e-mail: sudhakar.shet@nrel.gov
[b)]e-mail: yanfa.yan@nrel.gov
[c)]This author was an editor of this focus issue during the review and decision stage. For the *JMR* policy on review and publication of manuscripts authored by editors, please refer to http://www.mrs.org/jmr_policy
DOI: 10.1557/JMR.2010.0017

magnetron sputtering at varying RF power in mixed N_2 and O_2 ambient with low O_2 mass flow rate $\{[O_2/(N_2 + O_2)] = 10\%\}$. We also report on the synthesis of codoped ZnO:(Al,N) thin films at varying RF power with O_2 mass flow rate of $[(O_2/(N_2 + O_2)) = 25\%]$. We found that charge-compensated donor–acceptor codoping exhibits enhanced crystallinity and incorporates much higher N concentration in ZnO:(Al,N) thin films as compared to ZnO doped solely with N. As a result, ZnO:(Al,N) thin films presented improved PEC response, compared with ZnO:N films. Furthermore, we found that the N concentration in ZnO thin films can be effectively controlled by codoping by varying the RF power. This provides a general method for controlling N concentration in ZnO thin films grown by sputtering.

II. EXPERIMENTAL

Three sets of samples were deposited. One set of samples was deposited using a ZnO target in mixed N_2 and O_2 ambient with O_2 mass flow rate of $\{[O_2/(N_2 + O_2)] = 10\%\}$. We refer to this set of samples as ZnO:N. The second set of samples was deposited using ZnO–2wt% Al in mixed N_2 and O_2 ambient with O_2 mass flow rate of $\{[O_2/(N_2 + O_2)] = 10\%\}$. We refer to this set of samples as ZnO:(Al,N)(2). The third set of samples was deposited using ZnO–2wt%Al in mixed N_2 and O_2 ambient with O_2 mass flow rate of $\{[O_2/(N_2 + O_2)] = 25\%\}$ and is referred to as ZnO:(Al,N)(3). All the thin films were grown using a reactive RF magnetron sputtering system. F-doped SnO_2 (FTO; 20–23 Ω/Γ) coated transparent glasses were used as substrates. The distance between the target and substrate was 8 cm. The base pressure was below 5×10^{-6} Torr, and the working pressure for all synthesis was 2×10^{-2} Torr. The substrate was rotated at 30 rpm for uniform deposition of the film. Prior to sputtering, a presputtering process was performed for 30 min to eliminate any contaminants from the target. Sputtering was then conducted with different RF powers from 100 to 300 W at 100 °C. For comparison, ZnO and ZnO:Al film was deposited at an RF power of 300 W in pure Ar ambient. All samples were controlled to have a similar film thickness of about 1000 nm as measured by stylus profilometry.

The structure of synthesized films was characterized by x-ray diffraction (XGEN-4000, Scintag Inc.) operated with a Cu Kα radiation source at 45 kV and 37 mA. The N concentration in the thin films was evaluated by x-ray photoelectron spectroscopy (XPS). The ultraviolet-visible (UV-Vis) absorption spectra of the samples were measured by an n&k analyzer 1280 (n&k Technology, Inc., San Jose, CA) to investigate the optical properties of deposited thin films.

Photoelectrochemical measurements were performed in a three-electrode cell with a flat quartz-glass window to facilitate illumination to the photoelectrode surface.[19] The sputter-deposited films were used as the working electrodes with an active surface area of about 0.25 cm^2. Pt mesh and an Ag/AgCl electrode were used as counterelectrodes and reference electrodes, respectively. A 0.5 M Na_2SO_4 aqueous solution with a pH of 6.8 was used as the electrolyte for the PEC measurements, and scan rate of 5 mV/s was kept in this experiment. The PEC response was measured using a fiber-optic illuminator (150 W tungsten–halogen lamp) with a UV/infrared (IR) cut-off filter (cut-off wavelengths: 350 and 750 nm) and combined UV/IR and green bandpass filter [wave length: 538.33 nm, full width at half maximum (FWHM): 77.478 nm]. The light intensity was measured by a photodiode power meter. The total light intensity with the UV/IR filter only was fixed at 125 mW/cm^2.

Because our films were deposited on conducting substrates, measurements of electrical property by the Hall effect were not possible. Instead, the electrical properties were measured by Mott–Schottky plots, which were obtained by alternating current (ac) impedance measurements. The ac impedance measurements were carried out with a Solartron 1255 frequency response analyzer using the above three-electrode cells. Measurements were performed with an ac amplitude of 10 mV, and frequency of 5000 Hz under dark conditions and the ac impedances were measured in the potential range of −0.7 to 1.25 V (vs Ag/AgCl reference). The series capacitor–resistor circuit model was used for Mott–Schottky plots.[20,21]

III. RESULTS AND DISCUSSION

Figure 1 shows the XRD curves of the first set of samples: ZnO and ZnO:N films grown at different RF powers in mixed N_2 and O_2 ambient with O_2 mass flow rate of $\{[O_2/(N_2 + O_2)] = 10\%\}$. Dotted lines in the XRD

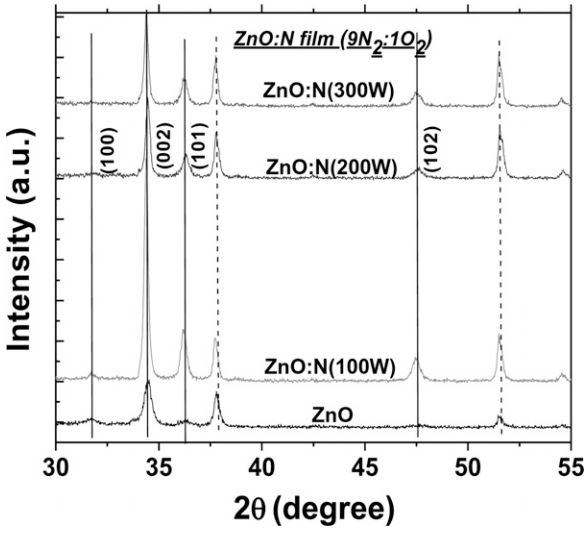

FIG. 1. X-ray diffraction curves of ZnO and ZnO:N films grown at different RF powers in mixed N_2 and O_2 ambient with O_2 mass flow rate of 10%.

plots indicate substrate peaks. The ZnO film exhibits poor crystallinity because of the low-temperature sputtering process. The ZnO:N film grown at 100 W showed better crystallinity than the pure ZnO film, despite the faster deposition rate. For ZnO growth, the ambient is pure Ar gas. For ZnO:N growth, the ambient is mainly N_2 with only 10% O_2. When the RF power was increased to 200 and 300 W, the crystallinity of the deposited films decreased. The ZnO:N films deposited at higher RF power grew faster compared with the deposition rate observed for deposition with 100 W RF power. The N concentrations in 100, 200, and 300 W samples were about 1, 1, and 2 at.%, respectively, as determined by XPS. It is known that a high concentration of dopant can deteriorate crystal structure. The average crystallite sizes were about 21, 42, 34, and 35nm for the ZnO, ZnO:N (100 W), ZnO:N(200 W), and ZnO:N(300 W), respectively, which were estimated by applying the Debye–Scherrer equation to our XRD data.

Figure 2(a) shows the optical absorption spectra of the ZnO and ZnO:N films grown at different RF powers. It is clearly seen that the absorption shifted increasingly to the longer-wavelength region as the RF power increased. This indicates that N incorporation in ZnO is increased as RF power increases.[22,23] Figure 2(b) shows the optical absorption coefficients of the ZnO and ZnO:N films grown at different RF powers. The direct electron transition from valence to conduction bands was assumed for the absorption coefficient curves, because ZnO films are known as direct-band gap materials.[1,23] The optical band gaps of the films were determined by extrapolating the linear portion of each curve. The band gap of the ZnO film is 3.26 eV, which is consistent with the results reported elsewhere.[24,25] The direct optical band gaps measured for ZnO:N films deposited at a substrate temperature of 100 °C gradually decreased to 3.13 eV as the RF power increased to 300 W.

Figure 3 shows the XRD curves of the second set of samples, ZnO:(Al,N)(2), ZnO, and ZnO:Al. The dotted lines indicate substrate peaks. It is seen that the ZnO:Al film exhibits poor crystallinity, likely because of the low deposition temperature and high RF sputtering process combined with pure Ar gas ambient. The ZnO:(Al,N)(2) film grown at 100 W shows better crystallinity than that of ZnO and ZnO:Al films, despite faster deposition rate. For pure ZnO growth, the ambient was Ar gas. For ZnO:(Al,N)(2) growth, the ambient is mainly N_2 with only 10% O_2. When the RF power was increased to 200 and 300 W, the crystallinity surprisingly increased and a significant amount of N was incorporated. Such significantly enhanced crystallinity is attributed to the charge-compensated donor–acceptor codoping. As the RF power was increased from 100 to 300 W, N incorporation in the films was increased. The concentrations of N in 100, 200, and 300 W samples were about 2, 4, and 5 at.%, respectively,

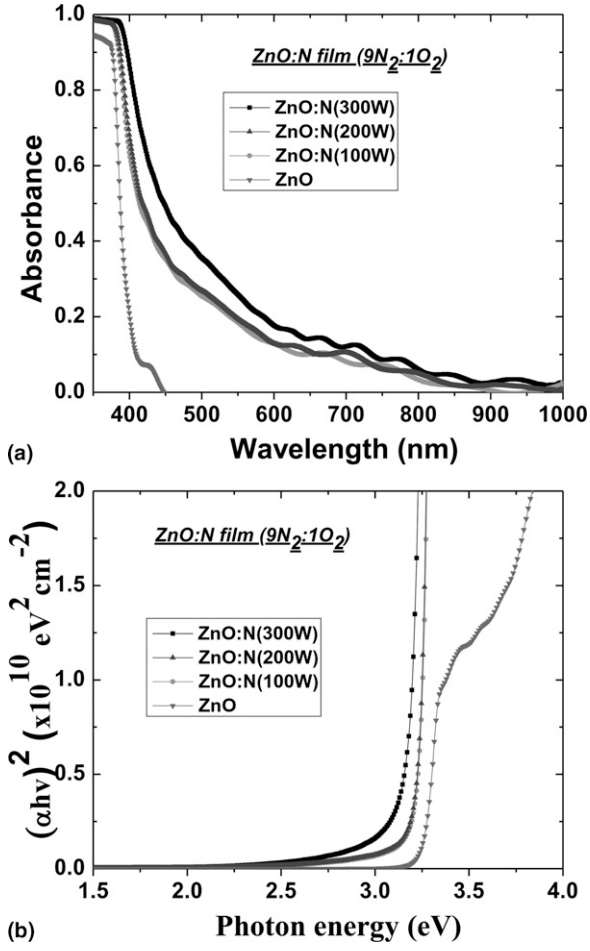

FIG. 2. (a) Optical absorption spectra of ZnO and ZnO:N films grown at different RF powers and (b) their corresponding optical absorption coefficients.

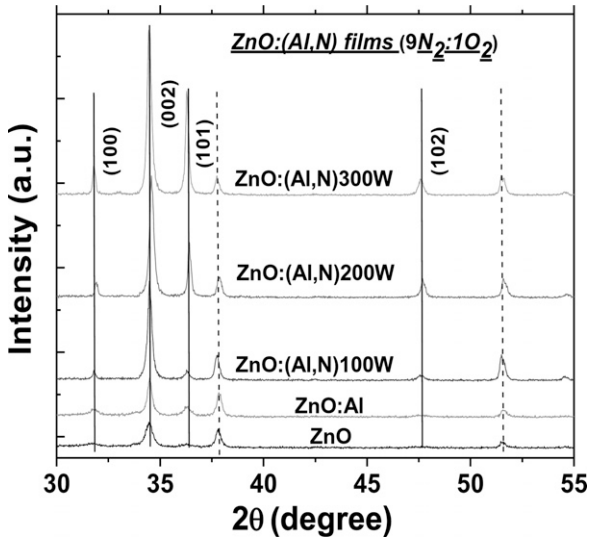

FIG. 3. X-ray diffraction curves of ZnO, ZnO:Al deposited at 300 W, and ZnO:(Al,N)(2) films grown at different RF powers in mixed N_2 and O_2 ambient with O_2 mass flow rate of 10%.

as determined by XPS. Applying the Debye–Scherrer equation to our XRD data, average crystallite sizes were estimated to be 21, 24, 32, 35, and 39 nm for the ZnO, ZnO:Al, ZnO:(Al,N)(2)(100 W), ZnO:(Al,N)(2)(200 W), and ZnO:(Al,N)(2)(300 W) films, respectively.

Figure 4 shows the optical absorption spectra of the ZnO, ZnO:Al, and ZnO:(Al,N)(2) films grown at different RF powers. It is seen that the ZnO:(Al,N)(2) films showed optical absorption in a much longer wavelength region compared with ZnO and ZnO:Al, indicating that a significant amount of N is incorporated in the films. The direct optical band gaps measured for ZnO:(Al,N)(2) films at 100 to 300 W drastically reduced from 3.13 to 2.02 eV, respectively. This significant band gap reduction is caused by enhanced N concentration incorporated in the films.

Figure 5 shows the XRD curves of the third set of samples, ZnO:(Al,N)(3) and ZnO and ZnO:Al deposited at 300 W. The dotted lines in the XRD plot indicate substrate peaks. It is clearly shown that as the RF power is increased from 100 to 300 W, crystallinity is enhanced greatly. Applying the Debye–Scherrer equation to our XRD data, crystallite sizes were estimated to be 21, 24, 28, 35, and 44 nm for the ZnO, ZnO:Al, ZnO:(Al,N)(2) (100 W), ZnO:(Al,N)(2)(200 W), and ZnO:(Al,N)(2) (300 W) films, respectively. The concentrations of N in 100, 200, and 300 W samples were about 1, 2, and 3 at.%, respectively, as determined by XPS. Compared with ZnO:(Al,N)(2) films grown in mixed N_2 and O_2 ambient with O_2 mass flow rate of 10%, ZnO:(Al,N)(3) thin films deposited in mixed N_2 and O_2 ambient with O_2 mass flow rate of 25% showed less N incorporation at respective RF powers. Figure 6 shows the optical absorption coefficient of the ZnO, ZnO:Al, and ZnO:(Al,N)(3) films grown at different RF powers. The direct optical band gaps measured for ZnO:(Al,N)(3) films at 200 and

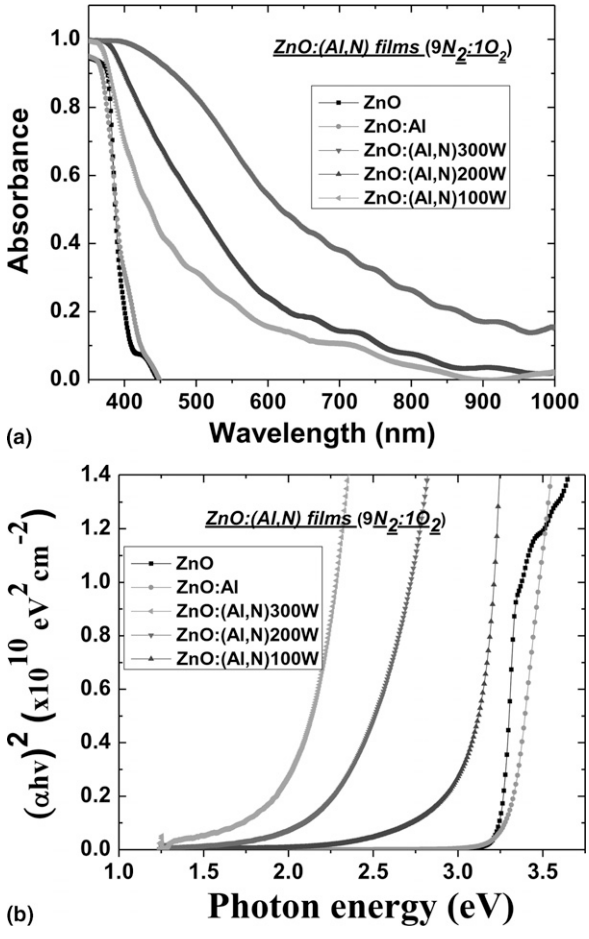

FIG. 4. (a) Optical absorption spectra of the ZnO, ZnO:Al, and ZnO:(Al,N)(2) films grown at different RF powers, and (b) their corresponding optical absorption coefficients.

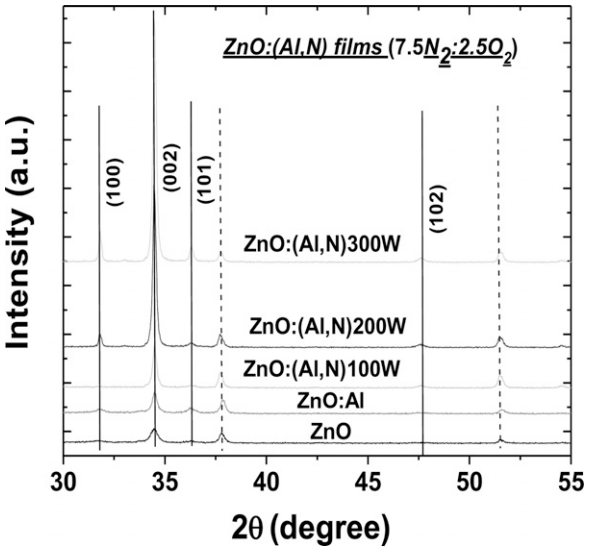

FIG. 5. X-ray diffraction curves of ZnO, ZnO:Al deposited at 300 W, and ZnO:(Al,N)(3) films grown at different RF powers in mixed N_2 and O_2 ambient with O_2 mass flow rate of 25%.

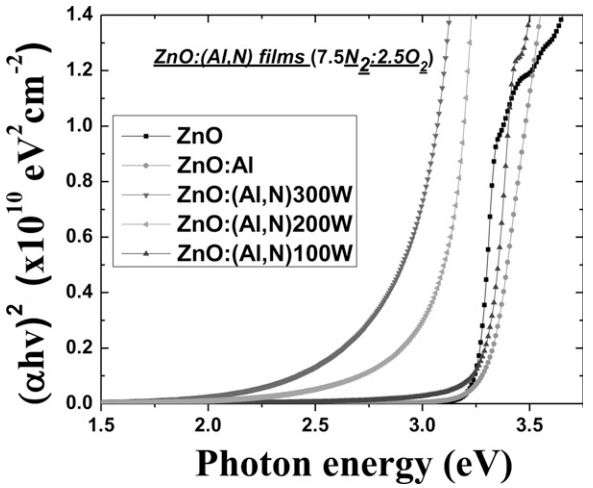

FIG. 6. The optical absorption coefficient of the ZnO, ZnO:Al, and ZnO:(Al,N)(3) films grown at different RF powers.

300 W are 3.13 and 2.9 eV, respectively. From these results, it is evident that with limited oxygen pressure, N incorporation in ZnO thin films can be controlled by varying the RF power during deposition.

Figures 7(a), 7(b), and 7(c) show Mott–Schottky plots of ZnO:N, ZnO:(Al,N)(2), and ZnO:(Al,N)(3) thin films, respectively. All the samples exhibited positive slopes, indicating n-type behaviors. Our previous studies[13,26–29] indicated that ZnO:N films deposited under a N_2/O_2 plasma showed n-type behaviors resulting from substitutional N_2 molecules that act as shallow double-donors. Perkins et al.[27] reported that a N_2/O_2 plasma can contain a significant fraction of N_2 molecules that can be incorporated into ZnO films, leading to the n-type behavior.

Figures 8(a), 8(b), and 8(c) show the photocurrent–voltage curves of the three sets of ZnO:N, ZnO:(Al,N)(2), and ZnO:(Al,N)(3) thin films, respectively, under illumination with the UV/IR filter. It clearly shows that the ZnO:Al:N(2) films exhibited enhanced

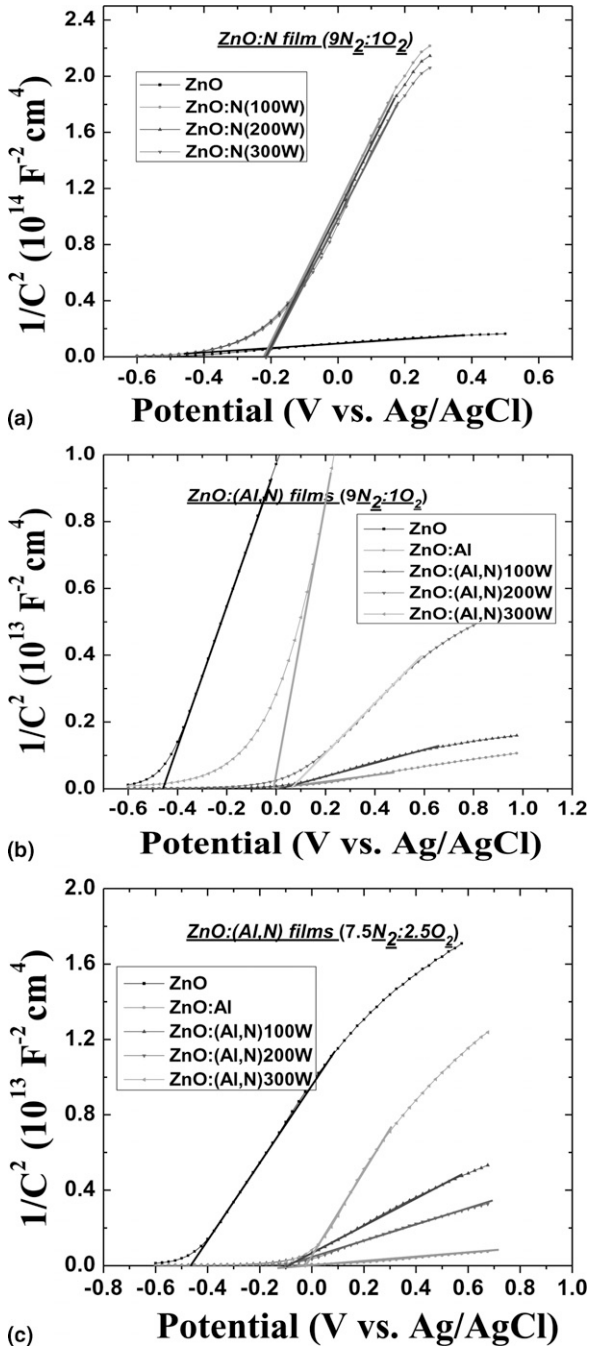

FIG. 7. Mott–Schottky plots of (a) ZnO:N, (b) ZnO:(Al,N)(2), and (c) ZnO:(Al,N)(3) thin films.

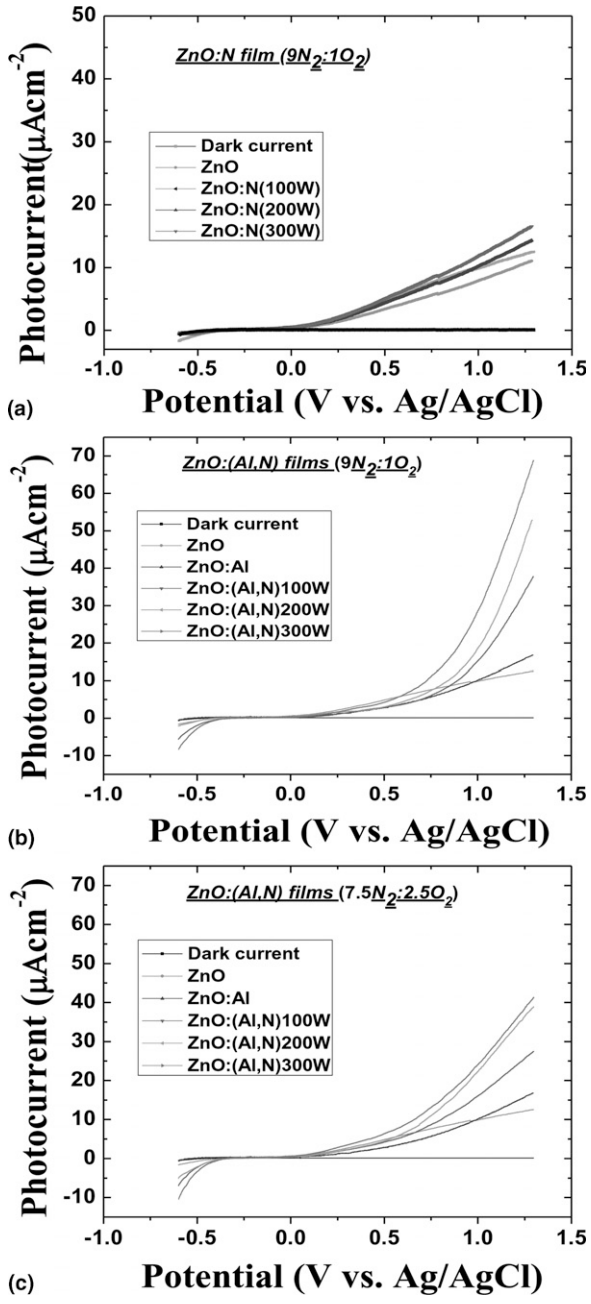

FIG. 8. Photocurrent–voltage curves of (a) ZnO:N, (b) ZnO:(Al,N)(2), and (c) ZnO:(Al,N)(3) thin films, under illumination with the UV/IR filter.

photocurrents, compared with the ZnO:(Al,N)(3) and ZnO:N films. At the potential of 1.2 V, the photocurrents were 5.2, 8.14, 10.09, and 12.1 μA/cm^2 for the ZnO, 100, 200, and 300 W ZnO:N films, respectively. At the same potential, the photocurrents were 14.6, 29.2, 40.1, and 54.3 μA/cm^2 for the ZnO:Al, 100, 200, and 300 W ZnO:(Al,N)(2) films, respectively. The photocurrents were 23.77, 33.64, and 35.66 μA/cm^2 for the 100, 200, and 300 W ZnO:(Al,N)(3) films, respectively. To investigate the photoresponses in the long-wavelength region, a green filter (wave length: 538.33 nm; FWHM: 77.478 nm) was used in combination with the UV/IR filter, as shown in Figs. 9(a)–9(c). The ZnO and ZnO:N films exhibited no clear photoresponse, because of their wide band gaps. The codoped ZnO:(Al,N) films exhibited much higher photocurrent than the ZnO:N film, despite much less light absorption. It indicates that a very high recombination rate of the photogenerated electrons and holes is present in the ZnO:N film, because of its inferior crystallinity and uncompensated charges. On the other hand, the codoped ZnO:(Al,N) film exhibited remarkably increased crystallinity, N incorporation, and charge compensation, which lead to enhanced photocurrent compared to the ZnO:N film. We encountered instability issues when the film is in contact with electrolytes. Nonetheless, the results clearly demonstrate that significantly reduced band gap, and enhanced photocurrents can be obtained with a controlled experimental parameter, i.e., charge-compensated donor–acceptor doping with low O pressure.

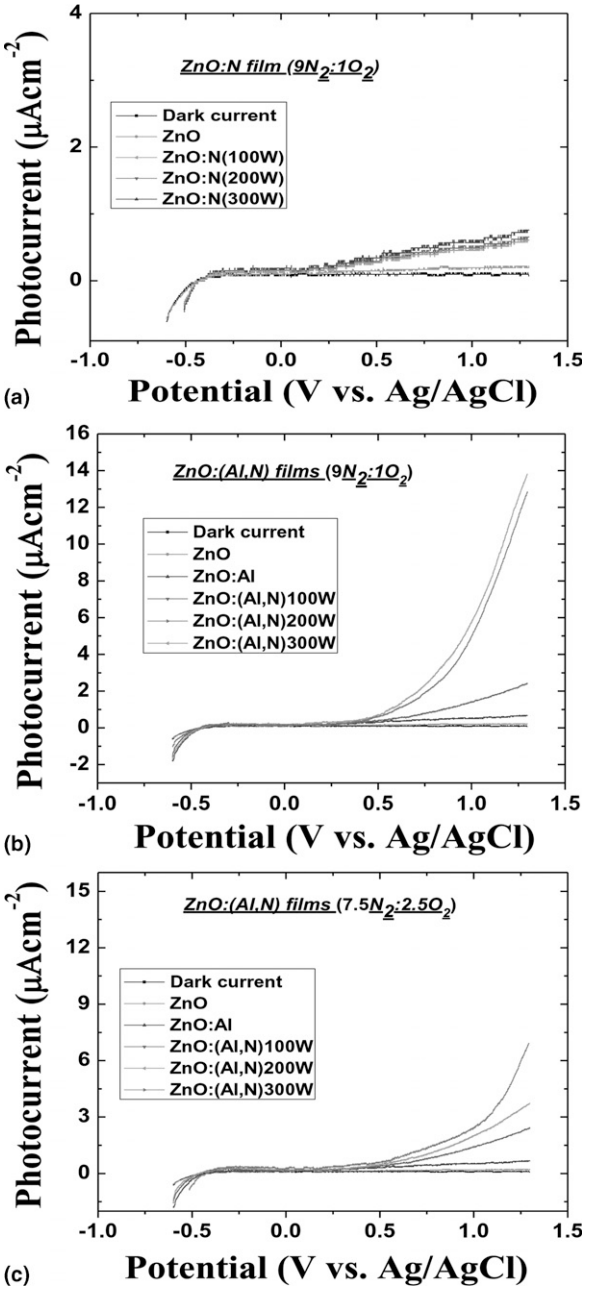

FIG. 9. Photocurrent–voltage curves of (a) ZnO:N, (b) ZnO:(Al,N)(2), and (c) ZnO:(Al,N)(3) thin films, under illumination with the combined green and UV/IR filters.

IV. CONCLUSIONS

ZnO:N and ZnO:(Al,N) thin films were synthesized on FTO substrates by reactive RF magnetron sputtering in mixed N_2 and O_2 ambient with different O_2 mass flow rates at 100 °C. Band gap narrowing of ZnO:N and ZnO:(Al,N) films was achieved by N incorporation. The N concentration in codoped ZnO:(Al,N), or the band gap of ZnO:(Al,N) thin films, can be controlled by the RF power and $O_2/(N_2 + O_2)$ mass flow rate ratio. The ZnO:(Al,N) films showed much higher N concentration than ZnO:N films doped solely by N. We found that codoped ZnO:(Al,N) films exhibited enhanced crystallinity compared with ZnO:N films. As a result, ZnO:(Al,N) films exhibited improved photocurrents than ZnO:N films grown with pure N doping, suggesting that charge-compensated donor–acceptor codoping could be a potential method to improve the efficiency of PEC water splitting using wide-band gap oxide materials.

ACKNOWLEDGMENT

This work was supported by the U.S. Department of Energy under Contract No. DE-AC36-08GO28308.

REFERENCES

1. M. Gratzel: Photoelectrochemical cells. *Nature* **414,** 338 (2001).
2. T. Bak, J. Nowotny, M. Rekas, and C.C. Sorrell: Photo-electrochemical hydrogen generation from water using solar energy. Materials related aspects. *Int. J. Hydrogen Energy* **27,** 991 (2002).
3. R. Asahi, T. Morikawa, T. Ohwaki, K. Aoki, and Y. Taga: Visible-light photocatalysis in nitrogen doped titanium oxides. *Science* **293,** 269 (2001).
4. S.U.M. Khan, M. Al-Shahry, and W.B. Ingler, Jr.: Efficient photochemical water splitting by a chemically modified n-TiO_2. *Science* **297,** 2243 (2002).

5. S. Sakthivel and H. Kisch: Angew: Daylight photocatalysis by carbon-modified titanium dioxide. *Chem. Int. Ed.* **42,** 4908 (2003).
6. T. Umebayashi, T. Yamaki, H. Itoh, and K. Asai: Bandgap narrowing of titanium dioxide by sulfur doping. *Appl. Phys. Lett.* **81,** 454 (2002).
7. K. Kakiuchi, E. Hosono, and S. Fujihara: Enhanced photoelectrochemical performance of ZnO electrodes sensitized with N-719. *J. Photochem. Photobiol., A* **179,** 81 (2006).
8. T.F. Jaramillo, S.H. Baeck, A. Kleiman-Shwarsctein, and E.W. McFarland: Combinatorial electrochemical synthesis and screening of mesoporous ZnO for photocatalysis. *Macromol. Rapid Commun.* **25,** 297 (2004).
9. K-S. Ahn, Y. Yan, and M. Al-Jassim: Band gap narrowing of ZnO:N films by varying rf sputtering power in O_2/N_2 mixtures. *J. Vac. Sci. Technol., B* **25,** L23 (2007).
10. D. Paluselli, B. Marsen, E.L. Miller, and R.E. Rocheleau: Nitrogen doping of reactively sputtered tungsten oxide films. *Electrochem. Solid-State Lett.* **8,** G301 (2005).
11. T. Yamamoto and H. Katayama-Yoshida: Solutions using a codoping method to unipolarity for the fabrication of p-type ZnO. *Jpn. J. Appl. Phys.* **38,** L166 (1999).
12. H. Matsui, H. Saeki, H. Tabata, and T. Kawai: Role of Ga for co-doping of Ga with N in ZnO films. *Jpn. J. Appl. Phys.* **42,** 5494 (2003).
13. Y. Yan, S.B. Zhang, and S.T. Pantelides: Control of doping by impurity chemical potentials: Predictions for p-type ZnO. *Phys. Rev. Lett.* **86,** 5723 (2001).
14. Z.W. Liu, S.W. Yeo, and C.K. Ong: Achieve p-type conduction in N-doped and (Al,N)-co-doped ZnO thin films by oxidative annealing zinc nitride precursors. *J. Mater. Res.* **22,** 2668 (2007).
15. J.G. Liu, Z.Z. Ye, F. Zhuge, Y.J. Zeng, B.H. Zhao, and L.P. Zhu: P-type conduction in N-Al co-doped ZnO thin films. *Appl. Phys. Lett.* **85,** 3134 (2004).
16. G.D. Yuan, Z.Z. Ye, L.P. Zhu, Q. Qian, B.H. Zhao, R.X. Fan, C.L. Perkins, and S.B. Zhang: Control of conduction type in Al- and N-codoped ZnO thin films. *Appl. Phys. Lett.* **86,** 202106 (2005).
17. Z-Z. Ye, F-Z. Ge, J-G. Lu, Z-H. Zhang, L-P. Zhu, B-H. Zhao, and J-Y. Huang: Preparation of p-type ZnO films by Al + N-codoping method. *J. Cryst. Growth* **265,** 127 (2004).
18. B.S. Li, Y.C. Liu, Z.Z. Zhi, D.Z. Shen, Y.M. Lu, J.Y. Zhang, X.W. Fan, R.X. Mu, and D.O. Henderson: Optical properties and electrical characterization of p-type ZnO films prepared by thermally oxiding Zn_3N_2 thin films. *J. Mater. Res.* **18,** 8 (2003).
19. S. Shet, K-S. Ahn, Y. Yan, T. Deutsch, K.M. Chrusrowski, J. Turner, M. Al-Jassim, and N.M. Ravindra: Carrier concentration tuning of bandgap-reduced p-type ZnO films by codoping Cu and Ga for improving photoelectrochemical response. *J. Appl. Phys.* **103,** 073504 (2008).
20. S-H. Kang, J-Y. Kim, Y. Kim, H-S. Kim, and Y-E. Sung: Surface modification of stretched TiO_2 nanotubes for solid state dye-sensitized solar cells. *J. Phys. Chem. C* **111,** 9614 (2007).
21. J. Akikusa and S.U.M. Khan: Photoelectrolysis of water to hydrogen in p-SiC/Pt and n-SiC/TiO_2 cells. *Int. J. Hydrogen Energy* **27,** 863 (2002).
22. M. Joseph, H. Tabata, and T. Kawai: P-type electrical conduction in ZnO thin films by Ga and N codoping. *Jpn. J. Appl. Phys.* **38,** L1205 (1999).
23. M. Futsuhara, K. Yoshioka, and O. Takai: Optical properties of Zinc oxynitride thin films. *Thin Solid Films* **317,** 322 (1998).
24. C.X. Xu, X.W. Sun, X.H. Zhang, L. Ke, and S.J. Chua: Photoluminescent properties of copper-doped zinc oxide nanowires. *Nanotech.* **15,** 856 (2004).
25. K.H. Kim, R.A. Wibowo, and M. Badrul: Properties of Al-doped ZnO thin films sputtered from powder compacted target. *Mater. Lett.* **60,** 1931 (2006).
26. K-S. Ahn, Y. Yan, S-H. Lee, T. Deutsch, J. Turner, C.E. Tracy, C. Perkins, and M. Al-Jassim: Photoelectrochemical properties of N-incorporated ZnO films deposited by reactive RF magnetron sputtering. *J. Electrochem. Soc.* **154,** B956 (2007).
27. C.L. Perkins, S.H. Lee, X. Li, S.E. Asher, and T.J. Coutts: Identification of N chemical states in N-doped ZnO via x-ray photoelectron spectroscopy. *J. Appl. Phys.* **97,** 034907 (2005).
28. K-S. Ahn, S. Shet, T. Deutsch, C-S. Jiang, Y. Yan, M. Al-Jassim, and J. Turner: Enhancement of photoelectrochemical response by aligned nanorods in ZnO thin films. *J. Power Sources* **176,** 387 (2008).
29. K-S. Ahn, Y. Yan, S. Shet, T. Deutsch, J. Turner, and M. Al-Jassim: Enhanced of photoelectrochemical responses of ZnO films through Ga and N codoping. *Appl. Phys. Lett.* **91,** 231909 (2007).